IEEE Asian Solid-State Circuits Conference
November 5 - 7, 2018/Tainan, Taiwan

A 2.4-GHz Single-Pin Antenna Interface RF Front-End with a Function-Reuse Single-MOS VCO-PA and a Push-Pull LNA

Kai Xu [1,2], Jun Yin [1], Pui-In Mak [1], Robert Bogdan Staszewski [2], Rui P. Martins [1,3]

1 - State-Key Laboratory of Analog and Mixed-Signal VLSI, University of Macau, Macau, China {E-mail: junyin@umac.mo}
2 - University College Dublin, Dublin, Ireland {E-mail: robert.staszewski@ucd.ie}
3 – On leave from Instituto Superior Técnico, Universidade de Lisboa, Portugal

***Abstract*—We propose a power-efficient sub-1V RF front-end (RFE) for 2.4GHz transceivers. It introduces the following innovations: 1) function-reuse single-MOS VCO-PA with full V_{DD} utilization while improving antenna-to-VCO isolation for better resilience to jammers; 2) a non-inverting transformer with a zero-shifting capacitor that suppresses the 2nd harmonic emission of the VCO-PA, and allows a single-pin antenna interface for both TX and RX modes; and 3) a push-pull LNA with passive gain boosting that reduces power consumption. Fabricated in 65nm CMOS, the RFE occupies merely 0.17mm^2. By scaling the supply voltage, the standalone VCO-PA exhibits a 20.8% (10.2%) power efficiency when delivering 0dBm (-10dBm) output. The LNA shows 11dB gain and 6.8dB NF while consuming 174μW.**

I. Introduction

Ultra-low-voltage (ULV) operation of IoT devices has been of great interest recently thanks to its feasibility of being self-powered by harvesting the ambient energy [1]-[2]. It is also well suited for Medical Body Area Network (MBAN) where low RF output power (e.g. −10dBm) is necessary. For the ubiquitous deployment sake, an ULV transmitter (TX) must be compatible with the mainstream IoT standards, such as Bluetooth low energy (BLE), while exhibiting good efficiency during the deep power back-off. It appears that the separate arrangement of the oscillator (e.g. VCO) and PA in conventional TXs cannot make that goal fully realizable. The recently introduced current-reuse PA-VCO [3] is incompatible with the ULV operation and has a limited output power due to the reduced voltage headroom. To overcome this, a six-port transformer of a recently introduced class-F DCO-PA [4] merges the DCO resonant tank with the PA matching network [Fig. 1(a)]. Yet, such a DCO-PA becomes extremely vulnerable to jammers appearing at the antenna. Besides, it requires off-chip filtering of HD_3 due to the 2nd impedance peak at the 3rd harmonic in class-F operation. In this paper, we propose a single-MOS VCO-PA [Fig. 1(b)] which improves jammer resilience and harmonic rejection. It utilizes the output matching transformer as a single-pin antenna interface for both TX and receiver (RX) modes, while offering passive gain boosting to the LNA, thus saving additional power. Fig. 2 depicts a complete diagram of the RFE.

II. Function-Reuse Single-MOS VCO-PA

To enhance the antenna-to-VCO isolation of the function-reuse VCO-PA architecture, we replace the drain-to-gate (D-to-G) feedback oscillation in [4] by an S(source)-to-G feedback. It is desirable here to maximize the coupling factor k_1 and L_g/L_s ratio to obtain a large loop gain and gate voltage swing, thereby lowering the power consumption and phase noise [5]. The swing at the source node must be lowered to attain better efficiency if the transistor is simultaneously reused as a PA, but that requires small L_s and k_1 values. Transformer T_1 comprises a series-wound 3 turns on top-metal (M9) as L_g (=2nH) and a parallel stack of 2 innermost turns of AP and M9 as L_s (=0.2nH). As such, we secure a moderate $k_1 = 0.5$ without much degradation of the tank quality factor. $V_{GB} + v_g$ biasing determines the conduction angle of the M_1 transistor and the use of a small $V_{GB} < 0.3$V stimulates M_1 to deliver a narrow current pulse to the output, further improving the power efficiency.

We chose a step-down (in TX mode) transformer T_2 with a small turns ratio of $n = 2{:}1$ for impedance enhancement at low output power (P_{out}) and high matching network efficiency [6]. A zero-shifting capacitor C_z between the two coils (L_o, L_d) of the non-inverting T_2 rejects the HD_2 of the single-MOS M_1. The transmission zero $f_z \propto \frac{\sqrt{n}}{\sqrt{L_o \cdot C_0}}$ for a certain k_2, wherein C_0 represents the inter-winding capacitance. Then, the proposed C_z artificially tunes C_0 shifting the zero notch down to $f_z = 2f_0$ where f_0 is ~2.4GHz. We verify the effectiveness of C_z with a simplified model (Fig. 3). $|V_{out}/V_d|$ shows a 26dB rejection at 4.8GHz at a cost of a sub-1dB passband loss. Even with a ±10% capacitance variation, this technique exhibits sufficient HD_2 rejection capability. Further, a high output impedance at $3f_0$ results from L_s and C_2 obstructing the 3rd-harmonic current.

III. Passive-Gain-Boosting Push-Pull LNA

In the TX mode, M_2 and M_3 are in cut-off and it is the parasitic capacitance at the drain of M_1 that can be reflected and absorbed into the output switched-capacitor bank C_o (3 bits). Similarly, when switching to the RX mode, M_1 in off state will present the main parasitic capacitance to the LNA, which can be compensated by altering C_o to a lower code for T_2 to retain a good frequency selectivity at 2.4GHz. The reverse signal flow in the RX mode allows the push-pull LNA to benefit from the passive gain of T_2. The input impedance matching of the LNA is aided by the supply and ground bondwire for inductive degeneration showing an input resistance: $R_{in} = \frac{g_m L_{bond}}{C_{gs}}$. To save die area, we place all active components underneath the passive transformers.

IV. Measurement Results

The RFE, fabricated in 65nm CMOS, occupies a compact active area of just 0.17mm^2 [Fig. 4(a)]. The HD_2 emission is −44.4dBm [Fig. 4(b)], which confirms the effectiveness of the zero-shifting C_z. The VCO-PA shows a 20.8% power efficiency when delivering P_{out}=0dBm at a 0.7V supply [Fig. 5(a)]. Phase noise is −126dBc/Hz at 2.5MHz offset [Fig. 5(b)]. Under a ULV supply of 0.3V, the VCO-PA sustains a relatively high efficiency >10% at -10dBm P_{out}. We verify the jammer resilience of the proposed VCO-PA to be far superior than in [4] through a −30dBm 5MHz-offset jammer [Fig. 5(c)]. The image spur detected at the output is −41dBm, which is at least 25dB better than in [4]. When the VCO-PA output pin switches to the LNA input, it exhibits 11dB gain with a noise figure (NF) of 6.8dB [Fig. 5(d)], while consuming 174μW at 0.5V.

V. Conclusions

This paper reports a 2.4GHz single-pin antenna-interface front-end featuring a single-MOS function-reuse VCO-PA and a push-pull LNA. The VCO-PA achieves high power efficiency even at a large power back-off while offering strong HD_2

978-1-5386-6413-1/18/$31.00 ©2018 IEEE

rejection by means of self-driven source-to-gate oscillation and zero-shifting capacitor, C_Z. Passive gain boosting and push-pull operation contribute significantly to the low power drain of LNA.

ACKNOWLEDGMENT

The authors acknowledge the support from: Macau FDCT SKL Fund, Univ. of Macau - MYRG2017-00185-AMSV, and Science Foundation Ireland 14/RP/I2921.

REFERENCES

[1] W. Yu *et al.*, "A 0.18V 382μW Bluetooth Low-Energy (BLE) Receiver with 1.33nW Sleep Power for Energy-Harvesting Applications in 28nm CMOS," *ISSCC*, pp. 414-415, Feb. 2017.

[2] M. Yuan *et al.*, "A 0.45V Sub-mW All-Digital PLL in 16nm FinFet for Bluetooth Low-Energy (BLE) Modulation and Instantaneous Channel Hopping Using 32.768kHz Reference," *ISSCC*, pp. 448-450, Feb. 2018.

[3] C. Li *et al.*, "Class-C PA-VCO Cell for FSK and GFSK Transmitters," *IEEE JSSC*, vol. 51, pp. 1537-1546, Jul. 2016.

[4] X. Peng *et al.*, "A 2.4-GHz ZigBee Transmitter Using a Function-Reuse Class-F DCO-PA and an ADPLL Achieving 22.6% (14.5%) System Efficiency at 6-dBm (0-dBm) P_{out}" *IEEE JSSC*, vol. 53, pp. 1495-1508, Jun. 2017.

[5] A. Ng *et al.*, "A 1-V 24-GHz 17.5-mW Phase-Locked Loop in a 0.18-μm CMOS Process," *IEEE JSSC*, vol. 41, pp. 1236-1244, Jun. 2006.

[6] M. Babaie *et al.*, "A Fully Integrated Bluetooth Low-Energy Transmitter in 28 nm CMOS With 36% System Efficiency at 3 dBm," *IEEE JSSC*, vol. 51, pp. 1547-1565, Jul. 2016.

[7] Y. Liu *et al.*, "A 1.9 nJ/b 2.4 GHz multistandard (Bluetooth Low Energy/Zigbee/IEEE802.15.6) transceiver for personal/body-area networks," *ISSCC*, pp. 446-447, Feb. 2013.

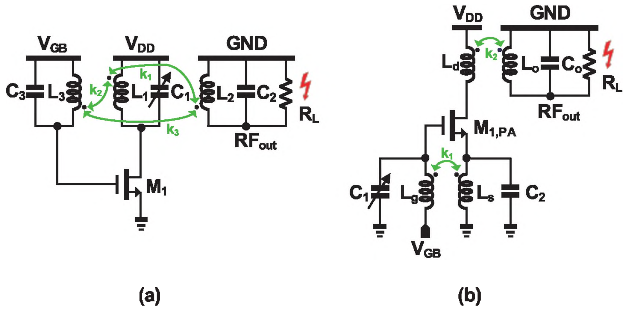

Fig. 1: Function-reuse DCO-PA: (a) in [4], and (b) in this work.

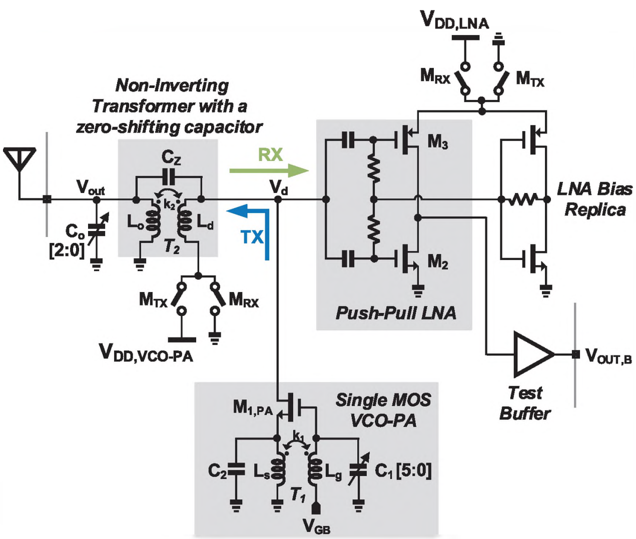

Fig. 2: Proposed single-pin antenna-interface RF front-end using a single-MOS VCO-PA and push-pull LNA.

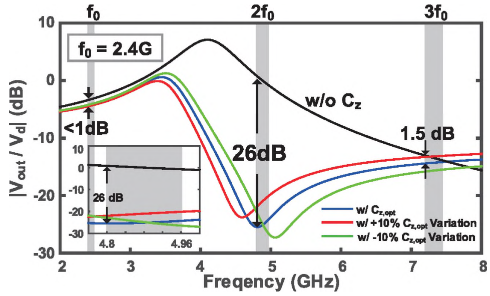

Fig. 3: Simulated HD_2 rejection with and without zero-shifting C_Z.

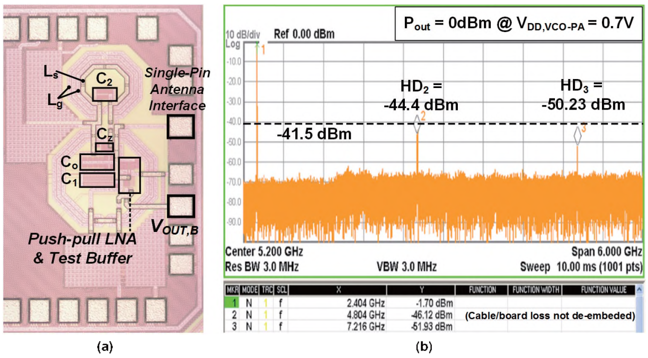

Fig. 4: (a) Die photo of the RFE. (b) Measured single-tone output spectrum.

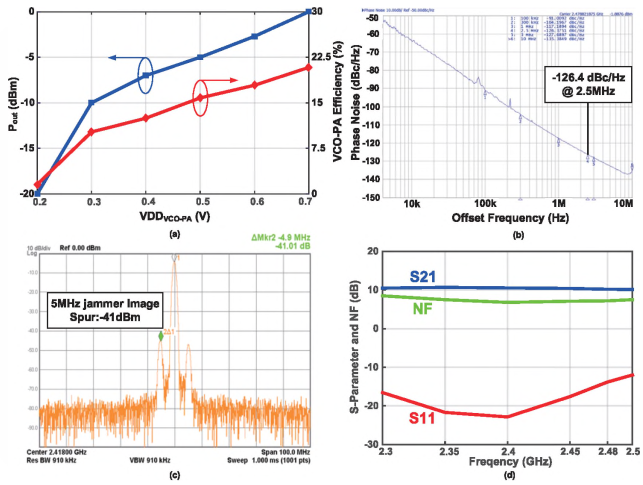

Fig. 5: Measured (a) VCO-PA P_{out} and power efficiency versus supply voltage; (b) Phase noise under P_{out} = 0dBm (c) VCO-PA under -30dBm jammer, and (d) LNA key performance metrics.

TABLE I. COMPARISON WITH STATE-OF-THE-ART VCO-PAS.

	ISSCC'13 [7]	JSSC'16 [3]		JSSC'16 [6]		JSSC'17 [4]		This work		
Supply Voltage (V)	1.2	1.2		0.5 + 1		0.3 to 0.7		0.3 to 0.7		
RF band (GHz)	2.4	2.4		2.4		2.4		2.4		
RF Power (dBm)	-10	-5	-1	-5	0	-5*	0	**-10**	**-5**	**0**
Power Consumption (mW) (VCO+Buffer+PA+Driver)	3.7	2.58	4.46	2.36	3.6	2.04	4.4	**0.98**	**2**	**4.8**
Efficiency (%)	2.7	12.2	17.9	13.4	28	15.5	22.6	**10.2**	**15.8**	**20.8**
Active Area (mm^2)	0.71	0.2		0.65		0.39		**0.17**		
HD2/HD3 @ P_{out} (dBm)	N/A	-50 / -47 @ 0dBm		<-40 / -40 @ - 1dBm		-43.2 / -47.6 @ 0dBm		**-44.4 / -50.2 @ 0dBm**		
VCO Phase Noise @ 2.5 MHz (dBc/Hz) / RF power	N/A	-129 @ -1dBm		-124		-125 @ 6dBm		-126 @ 0dBm		
5MHz jammer Image Spur @-30dBm interferer (dBm)	N/A	N/A		N/A		-13		**-41**		
Max P_{out} Variation under VSWR = 1.5 : 1 @ P_{out} (dBm)	N/A	N/A		N/A		2.1dB @ 6dBm		1.1dB @ 0dBm		
VCO-PA efficiency under VSWR = 1.5 : 1 @ P_{out} (%)	N/A	N/A		N/A		14 to 27.5 @ 6dBm		16 to 24.5 @ 0dBm		
Fully Integration	Yes	No		Yes		No		Yes		